Biomaterials 37 (2015) 164–173

Contents lists available at ScienceDirect

Biomaterials

journal homepage: www.elsevier.com/locate/biomaterials

TGFβ2 differentially modulates smooth muscle cell proliferation and migration in electrospun gelatin-fibrinogen constructs

Diana C. Ardila [a], Ehab Tamimi [a], Forest L. Danford [b], Darren G. Haskett [a], Robert S. Kellar [c, d, e], Tom Doetschman [f, g, h], Jonathan P. Vande Geest [a, b, h, i, *]

[a] Graduate Interdisciplinary Program of Biomedical Engineering, The University of Arizona, Tucson, AZ 85721, USA
[b] Department of Aerospace and Mechanical Engineering, The University of Arizona, Tucson, AZ 85721, USA
[c] Center for Bioengineering Innovation, Northern Arizona University, Flagstaff, AZ 86011, USA
[d] Department of Mechanical Engineering, Northern Arizona University, Flagstaff, AZ 86011, USA
[e] Department of Biological Sciences, Northern Arizona University, Flagstaff, AZ 86011, USA
[f] Department of Cellular and Molecular Medicine, The University of Arizona, Tucson, AZ 85721, USA
[g] Sarver Heart Center, The University of Arizona, Tucson, AZ 85724, USA
[h] BIO5 Institute for Biocollaborative Research, The University of Arizona, Tucson, AZ 85721, USA
[i] Department of Biomedical Engineering, The University of Arizona, Tucson, AZ 85721, USA

ARTICLE INFO

Article history:
Received 25 July 2014
Accepted 2 October 2014
Available online 22 October 2014

Keywords:
Electrospinning
Non-synthetic biopolymers
TGFB2
Smooth muscle cells
Migration
Proliferation

ABSTRACT

A main goal of tissue engineering is the development of scaffolds that replace, restore and improve injured tissue. These scaffolds have to mimic natural tissue, constituted by an extracellular matrix (ECM) support, cells attached to the ECM, and signaling molecules such as growth factors that regulate cell function. In this study we created electrospun flat sheet scaffolds using different compositions of gelatin and fibrinogen. Smooth muscle cells (SMCs) were seeded on the scaffolds, and proliferation and infiltration were evaluated. Additionally, different concentrations of Transforming Growth Factor-beta2 (TGFβ2) were added to the medium with the aim of elucidating its effect on cell proliferation, migration and collagen production. Our results demonstrated that a scaffold with a composition of 80% gelatin-20% fibrinogen is suitable for tissue engineering applications since it promotes cell growth and migration. The addition of TGFβ2 at low concentrations (≤1 ng/ml) to the culture medium resulted in an increase in SMC proliferation and scaffold infiltration, and in the reduction of collagen production. In contrast, TGFβ2 at concentrations >1 ng/ml inhibited cell proliferation and migration while stimulating collagen production. According to our results TGFβ2 concentration has a differential effect on SMC function and thus can be used as a biochemical modulator that can be beneficial for tissue engineering applications.

1. Introduction

The failure or loss of tissue is one of the most common and costly problems in medicine today [1–3]. The main treatments for these disorders are tissue transplants and surgical reconstruction [1,2,4]. The principal limiting factors for these transplants include donor availability, immunocompatibility of the donated tissue with the host body, and the suitability and availability of alternative tissue, especially in the case of autotransplant [1,5]. Surgical reconstructions are limited by the amount of viable and healthy tissue surrounding the wound, and many times requires a graft transplantation [1,4]. Tissue engineering is an advancing interdisciplinary field that applies an engineering approach towards the development of scaffolds that replace, restore, and improve diseased tissue [4,5]. The goal of tissue engineering is to fabricate new, physiological, and viable tissue substitutes that can be integrated into the patient to successfully restore function [1,2,4]. To enable injured tissue to regenerate, tissue engineered scaffolds must mimic native tissue, which is mainly comprised of cells supported by an extracellular matrix (ECM) and signaling molecules such as growth factors and cytokines [3,5]. Tissue engineered scaffolds must promote cell–biomaterial interactions, cell growth, and ECM deposition while also encouraging nutrient transport and gas exchange to promote cell proliferation while minimizing

* Corresponding author. Aerospace and Mechanical Engineering, The University of Arizona, 1130 N. Mountain, PO Box 210119, Tucson, AZ 85721-0119, USA. Tel.: +1 520 621 2514; fax: +1 520 621 8191.
E-mail address: jpv1@email.arizona.edu (J.P. Vande Geest).

http://dx.doi.org/10.1016/j.biomaterials.2014.10.021
0142-9612/

inflammation and toxicity [1–4]. In addition, scaffold degradability rate needs to be comparable to that of tissue regeneration [1–4]. Biopolymers are widely used to fabricate tissue engineered grafts due to their mechanical properties, biocompatibility, biodegradability, and chemical versatility [4]. Synthetic biodegradable polymers used in tissue engineering can mimic the mechanical properties of native tissue [6,7]. However, these polymers differ from native biopolymers in the ECM, and therefore have different binding sites, making cell attachment and migration difficult [8]. Additionally, synthetic polymers are often hydrophobic, which limits the absorption of culture medium, and consequently, cell proliferation becomes slow and poor [9,10]. Recently, naturally derived biopolymers have received increased attention in tissue engineering applications. They are mainly comprised of proteins derived from the ECM of a specific tissue, which has been shown to provide better physiological support for cell attachment and growth [8]. In contrast to synthetic biopolymers, natural biopolymers are mainly hydrophilic, facilitating the absorption and diffusion of nutrients, while also providing specific interaction sites with cells, thus enhancing cell adhesion and proliferation [7,8,11–13].

Multiple techniques have been applied to fabricate scaffolds suitable for tissue replacement. Among these techniques, electrospinning has been extensively used to create fibrous scaffolds, showing promising results for tissue engineering applications [7,14]. Electrospinning produces non-woven meshes containing fibers ranging in diameter from tens of microns to tens of nanometers, generating matrices that mimic the natural ECM microstructure [14]. A more detailed explanation of the electrospinning process can be found in Rim et al., 2013 [15]. Briefly, polymers are dissolved in an organic solvent to create a polymeric solution. The solution is then loaded into a syringe with a dispensing blunt tip needle attached. The syringe is placed into a syringe pump to regulate flow through the needle. A high voltage is then applied to the needle, which is placed opposite of the grounded metallic target to create a differential voltage potential. The electric field then pulls the polymer out of the syringe tip in the form of fibers, which get deposited on the metallic target [11,15].

Tissue engineered scaffolds are meant to provide structural integrity for cell growth and facilitate the formation of new tissue from the initially seeded cells [8]. These cells can be derived from primary tissue or cell lines [13]. For tissue engineering purposes, cells should be highly proliferative, easy to harvest, and have the necessary specialized functions to replace the injured tissue [1,13]. The gene expression of cells in engineered tissues can be regulated by various signaling molecules including platelet derived growth factor (PDGF), fibroblast growth factor (FGF), activin A, angiotensin II (AngII), insulin growth factor (IGF), transforming growth factor (TGFβ), among others [8]. Each of them has a particular effect on the cell phenotype and can be impregnated in the scaffold, which allows for selective improvement of cell function [8].

In this study, non-synthetic biopolymer-based planar scaffolds were created through the electrospinning of gelatin and fibrinogen at different mass ratios [16]. The scaffolds were seeded with porcine aortic smooth muscle cells (PAOSMCs), and cell proliferation and scaffold infiltration were assessed to determine the most suitable substrate for SMC attachment, growth, and migration. The experimental ratios between gelatin and fibrinogen were selected based on the study of Balasubramanian et al., 2013 [16], where the authors demonstrated that a scaffold composed of 80% gelatin-20% fibrinogen supported cardiac myocyte culture better than pure fibrinogen scaffolds. Additionally, the author's findings suggested that the addition of gelatin in a higher proportion to the polymeric solution, can enhance the mechanical properties of the scaffold [16]. However, the authors did not test cell behavior in 100% gelatin scaffolds. In this study, we compared cell proliferation and migration in scaffolds with compositional percentages of 100% gelatin; 80% gelatin-20% fibrinogen; and 50% gelatin-50% fibrinogen. Since TGFβ2 is important for pharyngeal arch artery remodeling [17] and for ECM remodeling in heart valvulogenesis [18], it was added to the culture medium at different concentrations to assess its effect on SMC proliferation, migration, and collagen production in the tissue engineered scaffolds. This research evaluates the suitability of a biomaterial for vascular tissue engineering applications and also provides insight into the use of different concentrations of exogenous TGFβ2 as a signaling control factor to promote/decrease SMCs growth and migration as well as collagen deposition in the supporting material.

2. Materials and methods

2.1. Smooth muscle cell isolation

Smooth muscle cells (SMCs) were isolated from porcine aorta using the explant method reported in Gallicchio et al., 2001; and Gotlieb & Boden, 1984 [19,20]. Briefly, aortas were obtained from the University of Arizona Meat Science Laboratory 10–20 min post-mortem. The adventitia and intima were removed from the explants in sterile conditions. The medial layer was cut into small pieces, and the explants were placed in 60 mm petri dishes containing 5 ml of Dulbecco's Modified Eagle Medium (DMEM) from Gibco® (Life technologies™, USA) supplemented with 10% Fetal Bovine Serum (FBS) from GemCell™, 100U/ml of penicillin, 100 μg/ml of streptomycin, 5 μg/ml of amphotericin B (Fungizone), and 25 mM HEPES from Gibco®(Life technologies™, USA). The culture medium was changed every other day and cultures were maintained in a humidified environment at 37°C and 5% CO_2. Cell outgrowth from the explants was observed after two weeks. Cell identity was confirmed by immunocytochemistry (ICC) on cells cultured on glass coverslips after the second passage, using double immunostaining by primary monoclonal antibodies mouse anti-alpha smooth muscle actin (ab7817; Abcam, USA) and rabbit anti-calponin (ab46794; Abcam, USA). Primary antibodies were conjugated with secondary antibodies Alexa Fluor® 488 goat anti mouse (Life Technologies™, USA) and goat anti-rabbit Cy5 (ab97077; Abcam, USA). Cell nuclei were counterstained using VECTSHIELD® mounting media containing 4',6-diamidino-2-phenylindole (DAPI) from Vector Laboratories, USA. For all other experiments performed, cells from passages 4–6 were used.

2.2. Scaffold fabrication

Gelatin-Fibrinogen flat sheet scaffolds were created by electrospinning. Gelatin extracted from porcine skin and fraction I bovine fibrinogen (Sigma–Aldrich, USA) were mixed at three different percentages: 100% gelatin (100 G), 80% gelatin-20% fibrinogen (80:20 G:F) and 50% gelatin-50% fibrinogen (50:50 G:F) [16]. The polymeric blends were dissolved in 1,1,1,3,3,3-Hexafluoro-2-propanol (HFP) (Sigma–Aldrich, USA) to create a 10% (w/v) solution under constant stirring. The solutions were loaded into a 5 ml BD syringe with a 23 gauge stainless steel dispensing blunt tip needle (CML supply, USA) attached. The syringe was then loaded onto a NE-1000 single syringe pump (New era pump systems inc., USA) set to a pumping rate of 100 μl/min. The distance from the needle tip to the target was 8 cm. The polymeric solutions were electrospun at a high voltage of 15 kV, onto glass coverslips attached to a metallic target to create fine fibers. The resultant flat sheets were crosslinked in 25% glutaraldehyde (Sigma–Aldrich, USA) in vapor phase for 24 h. The glutaraldehyde was then removed in a convection oven for 24 h at 42°C. Additionally, membranes were rinsed with deionized water to remove any crosslinker residues and uncrosslinked gelatin.

2.3. Cell culture

Membranes were sterilized with 70% ethanol solution for 4 h, rinsed with sterile PBS (Gibco®, Life technologies™, USA), placed under UV light for 2 h, and conditioned in culture medium for 30 min. After conditioning, the flat sheets were transferred to 6-well plates containing 3 ml of culture medium per well; having one scaffold per well. Each flat sheet was positioned flat on the bottom of the well. Scaffolds were seeded by dispensing a solution of detached SMCs on the flat sheets at a concentration of 1×10^6 cells/ml into each well. Cultures were maintained at 37°C and 5% CO_2 in a humidified atmosphere. Culture medium was changed every other day. After 2 and 7 days of culture, proliferation and infiltration were evaluated. All the experiments had 6 replicates ($n = 6$).

2.4. Evaluation of cell proliferation

To quantify cell proliferation, a proliferation assay was performed on every flat sheet. A sample with a surface area of approximately 35 mm^2 was cut from each scaffold and then placed in a well of a 96-well plate containing 100 μl of culture medium. Viable cell number was determined by the bioreduction of 3-(4,5-Dimethyl-thiazol-2yl)-5-(3-carboxymethoxyphenyl)-2-(4-sulfophenyl)-2H-

tetrazolium contained in the CellTiter 96® AQueous One Solution Cell Proliferation Assay (Promega, USA) following the manufacturer's instruction. Absorbance was read at 490 nm in a Synergy H1 plate reader from BioTek®. Statistical significance was assessed using one way ANOVA.

2.5. Cell infiltration imaging

The Advanced Intravital Microscope (AIM) for multiphoton imaging at the University of Arizona's BIO5 institute was used to observe the total cell migration along the scaffold depth [21,22]. The AIM is an Olympus BX51 upright laser-scanning microscope coupled to a Coherent 120-fs tunable pulsed Titanium-Sapphire laser (Santa Clara, CA). For this study an Olympus XLUMPLFL 20× water immersion objective with a numerical aperture of 0.9 was used. Incident light was focused on the sample and the epifluorescent signal was collected over a 400 × 400 μm field of view at 5 μm steps, imaging through the flat sheet to a depth of approximately 150 μm. For cell imaging, the sheets were treated for 24 h with VECTASHIELD® mounting medium with DAPI (Vector Laboratories, USA) to stain cell nuclei. The laser was centered at $\lambda = 700$ nm to excite DAPI; the epifluorescent light was first split with a 505 nm dichroic mirror and then collected through a 460/80 bandpass filter. The wavelength of the laser was then centered at $\lambda = 920$ nm to generate a strong autofluorescent signal from gelatin and fibrinogen. This epifluorescent signal was split with a 580 nm dichroic mirror and collected through a 550/88 bandpass filter. The optical path was chosen to maximize discrimination between gelatin/fibrinogen and DAPI 2PEF. This set up allows us to sequentially capture the same image volume, mitigating any need to colocalize. Two representative regions of the scaffold were imaged and infiltration was estimated by image analysis. The image volumes from DAPI and autofluorescence were merged to visualize the 3D cell location in the flat sheet. Infiltration was calculated as the average percentage of cell migration through the flat sheet (from the top surface to the bottom) relative to the flat sheet thickness.

2.6. Scaffold porosity and fiber diameter

Scaffold characterization was performed on the 2PEF image volume described above to ensure that just fibers were being evaluated. Porosity was calculated by first creating a maximum intensity projection (MIP) of the image volume, manually thresholding the resulting MIP, binarizing the image volume based on the chosen threshold value (of the MIP image), selecting a smaller representative image volume region of interest (to avoid underestimation due to the surface of the sheet not being perfectly flat and loss of signal through the depth), and then dividing the total number of black pixels in the user defined image volume divided by the total number of pixels. The fiber diameter was calculated by manually measuring the diameter of 20 randomly selected fibers per scaffold via freehand lines superimposed over slices from the thresholded image volume in ImageJ. The above described process was performed by 3 separate individuals to minimize any user bias and capture a representative population of fiber diameters [23].

2.7. Addition of exogenous TGFβ2

Flat sheets composed of 80:20 G:F were seeded with PAOSMCs at a concentration of 1×10^6 cell/ml in 6-well plates, as previously described. Exogenous TGFβ2 (R&D Systems, USA) was added to the culture medium at different concentrations (0.05, 0.1, 0.5, 1, 3, 5, and 10 ng/ml). The absence of TGFβ2 in one of the cultures was used as a control. The cultures were maintained in a humidified atmosphere at 37 °C and 5% CO_2. Culture medium was changed every alternate day, adding every time the predetermined concentration of exogenous TGFβ2. After 7 days, cell proliferation and infiltration were assessed. Additionally, collagen production was analyzed. All experiments had 6 replicates, and statistical significance was evaluated using a one way ANOVA.

2.8. Analysis of collagen content

Collagen concentration was examined in the culture medium as well as in the flat sheets, using a soluble collagen assay (QuickZyme Biosciences, USA). To determine the collagen concentration dissolved in culture media at day 6 of culture, the membranes were rinsed with sterile PBS and placed in new 6-well plates containing fresh medium. Exogenous TGFβ2 was added to the predetermined concentration. After 24 h, the medium was aspirated and centrifuged at 3000× *g* to remove cell debris. The assay was carried out according to the manufacturer's instructions. Absorbance was read at 540 nm in a Synergy H1 plate reader from Biotek®. In addition to running a collagen assay for the cell media, an assay was also performed for the flat sheets using a sample with a surface area of approximately 1.8 cm^2. The samples were rinsed with sterile PBS, homogenized in a collagen solubilization buffer (0.5 M acetic acid, 5 mM EDTA, and 0.05 g pepsin/100 g tissue) using the TissueRuptor® (Quiagen, Germany) and incubated under constant stirring. After 24 h, the collagen dissolved in the buffer was analyzed using a QuickZyme soluble collagen assay, following the manufacturer's guidance. Absorbance was read at 540 nm in a Synergy H1 plate reader from Biotek®.

3. Results

3.1. Scaffold characterization

The results from the three independent analysts were averaged to calculate the porosity and fiber diameter for each scaffold. For 100 G, the averaged porosity was 70.6% ± 14% and the fiber diameter 3.57μm ± 1.66 μm. The results for the porosity in 80:20 G:F were 45.4% ± 1.5% and 3.82μm ± 2.04 μm for the fiber diameter. In the 50:50 G:F the porosity was calculated as 62.3% ± 5.0% and the fiber diameter as 4.48μm ± 1.56 μm.

3.2. Cell culture, proliferation and infiltration in electrospun scaffolds with different compositions

Identity of the isolated SMCs was confirmed by ICC. The cells expressed both alpha-smooth muscle actin and calponin (Fig. 1). These markers are specific to SMCs expressing a contractile phenotype [24–28]. The cells also presented an elongated morphology typical of contractile SMCs [29]. There was a significant increase ($p < 0.05$) in cell count from 2 to 7 days in all three types of scaffolds (Fig. 2). After 2 and 7 days of cell seeding, SMCs showed more proliferation in 80:20 G:F scaffolds than in 50:50 G:F and 100 G. A significant effect on cell number ($p < 0.05$) was identified after 2 days in culture comparing 80:20 G:F with 50:50 G:F ($1.79 \times 10^5 \pm 2.46 \times 10^4$ vs. $1.2 \times 10^5 \pm 1.12 \times 10^4$). Also, cell count was higher in 80:20 G:F compared with 100 G, however no significant difference identified ($1.79 \times 10^5 \pm 2.46 \times 10^4$ vs. $1.43 \times 10^5 \pm 2.73 \times 10^4$). After 7 days in culture a significant increase in cell number was found for 80:20 G:F compared to 50:50 G:F ($5.28 \times 10^5 \pm 4.6 \times 10^4$ vs. $5.04 \times 10^5 \pm 4.60 \times 10^4$, $p < 0.05$), and in 80:20 G:F compared to 100 G ($5.28 \times 10^5 \pm 4.6 \times 10^4$ vs. $3.81 \times 10^5 \pm 7.1 \times 10^4$, $p < 0.05$).

In Fig. 2, it can also be observed that 2 days post seeding, the 100 G sheets have on average more cells attached than 50:50 G:F sheets. In contrast, at 7 days 100 G scaffolds showed the lowest cell proliferation of all scaffolds.

Migration results (Fig. 3a) showed a significant increase ($p < 0.05$) in cell movement through the scaffold depth from 2 to 7 days after cell seeding in all three construct formulations, being greater the percentage of scaffold infiltration after 7 days in culture.

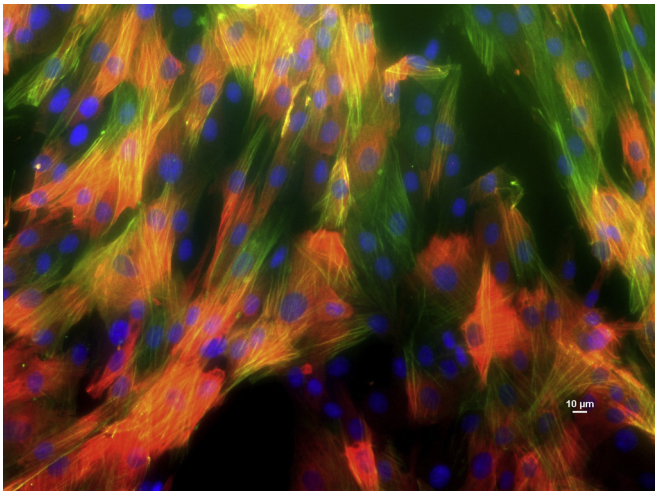

Fig. 1. Double immunostaining of alpha-smooth muscle actin (green) and calponin (red) in smooth muscle cells isolated from a porcine aorta, cultured in coverslips after the second passage. Cell nuclei were counterstained with DAPI (blue). Image taken at a magnification of 20×.

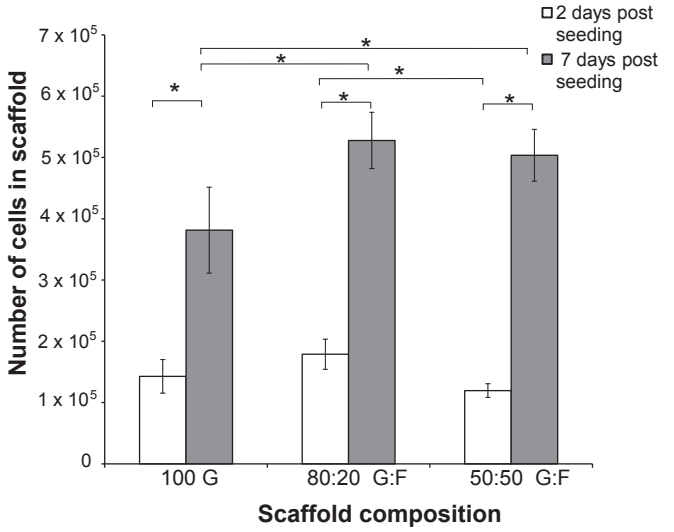

Fig. 2. Cell Proliferation results after 2 (white) and 7 (gray) days post seeding in 100 G, 80:20 G:F, and 50:50 G:F electrospun scaffolds. Average cell number per scaffold is reported for the two time points. Error bars shown are standard deviation (*$p < 0.05$; $n = 6$).

For the 100 G scaffolds, the average percentage of cell migration through the scaffold depth after 2 and 7 days was 36.16% ± 2.07% and 91.66% ± 1.7%, respectively. For the 80:20 G:F scaffolds, the average percentage of cell migration after 2 and 7 days was 45.36% ± 2.85% and 90.96% ± 1.41%, respectively. For 50:50 G:F the average percentage of cell migration after 2 and 7 days was 35.53% ± 1.04% and 97.66% ± 2.05%, respectively. In Fig. 3b, a composite from multiphoton imaging of the 80:20 flat sheets 7 days post SMCs seeding is shown. It is possible to observe that cells (DAPI 2PEF, nuclei shown in blue) have migrated down through the material fibers (gelatin and fibrinogen autofluorescence 2PEF, fibers shown in green).

3.3. Effect of exogenous TGFβ2 in cell proliferation, migration, and collagen production

Exogenous TGFβ2 at concentrations ≤1 ng/ml had a positive effect on cell count (proliferation) compared to the control (Fig. 4). At concentrations >1 ng/ml, TGFβ2 suppressed cell growth. The largest number of cells in scaffolds was found in cultures where TGFβ2 was added to the medium at a concentration of 0.1 ng/ml with a significant main effect ($p < 0.05$) compared to control ($3.24 \times 10^5 \pm 2.81 \times 10^4$ vs. $2.31 \times 10^5 \pm 5.75 \times 10^4$). The lowest number of cells growing in the scaffolds was obtained with TGFβ2 at 5 ng/ml and 10 ng/ml with a significant reduction compared to control ($3.24 \times 10^5 \pm 2.81 \times 10^4$ vs $1.62 \times 10^5 \pm 2.56 \times 10^4$, $p < 0.05$ for the control vs 5 ng/ml TGFβ2, and $3.24 \times 10^5 \pm 2.81 \times 10^4$ vs. $1.76 \times 10^5 \pm 8.78 \times 10^3$, $p < 0.05$ for the control vs 10 ng/ml TGFβ2).

A significant increase ($p < 0.05$) in SMCs migration was found when TGFβ2 was at 0.1 ng/ml compared to control (99% ± 0.5% vs. 83.88% ± 0.8%) and a significant reduction ($p < 0.05$) in cell migration in 10 ng/ml TGFβ2 samples compared to control (14.28% ± 1.14% vs. 83.88% ± 0.83. Representative multiphoton images of the scaffolds for TGFβ2 concentrations of 0.1 ng/ml and 10 ng/ml are shown as composites in Fig. 5b and c, respectively. The 80:20 G:F sheets are displayed in green (autofluorescence 2PEF) and cell nuclei in blue (DAPI 2PEF). The left side of each figure panel is a 3D rendering of the scaffold where the *y* plane of the green channel was clipped to facilitate cell location visualization. The right panel is the *xz* view of the 3D render where the cell position

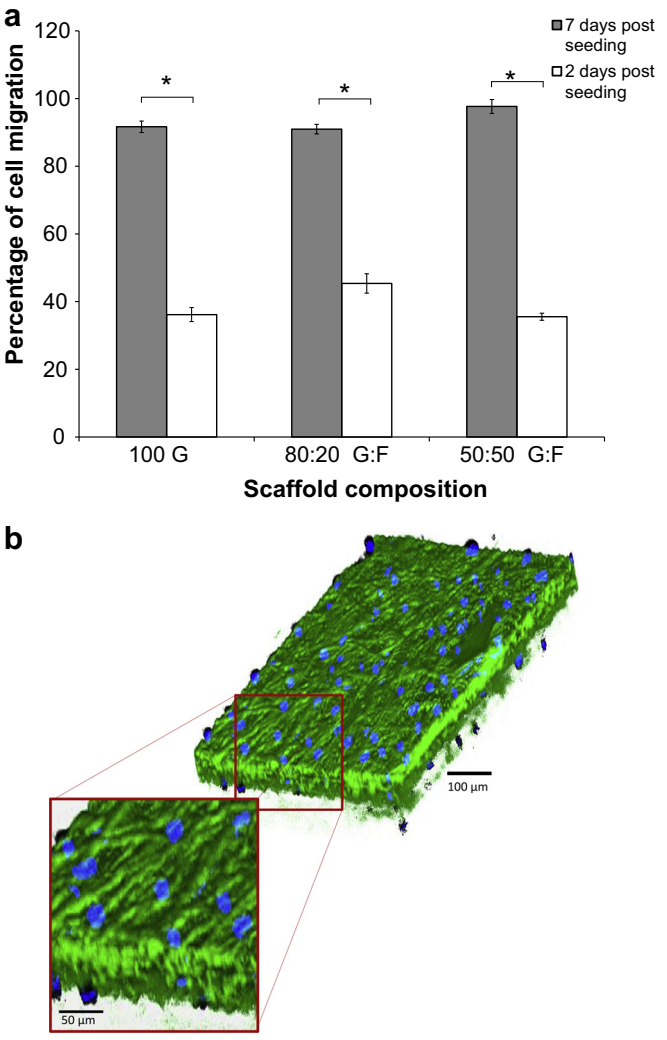

Fig. 3. a) Cell infiltration results after 2 (white) and 7 (gray) days post seeding in 100 G, 80:20 G:F, and 50:50 G:F electrospun scaffolds. Average percentage of migration through the scaffold depth is reported for the two time points. Error bars shown are standard deviation (*$p < 0.05$; $n = 2$). b) Representative multiphoton image of an 80:20 G:F flat sheet with cells after 7 days in culture. The material fibers are shown in green, and cell nuclei in blue. Image was acquired at a magnification of 20×.

along the *z* axis is shown. Fig. 5b shows how the cells migrated through the entire scaffold depth as they are located in different positions along the *z* axis. Fig. 5c demonstrates that the cells subjected to higher TGFβ2 concentrations displayed limited migration.

Fig. 6a shows the results for the collagen dissolved in growth media that was produced from day 6 to day 7. The amount of collagen was normalized by the number of cells in the flat sheet. The largest amount of collagen was produced when the concentration of TGFβ2 was 10 ng/ml (8.89×10^{-5} µg/cell ± 5.63×10^{-5} µg/cell), and the least amount of collagen was obtained when the TGFβ2 was 0.1 ng/ml (3.17×10^{-5} µg/cell ± 1.35×10^{-5} µg/cell), which is lower than the control (4.37×10^{-5} µg/cell ± 2.38×10^{-5} µg/cell). A similar tendency was obtained when the collagen was measured in the scaffolds (Fig. 6b). The largest amount of collagen in the flat sheets was obtained with a concentration of TGFβ2 of 10 ng/ml (2.19×10^{-3} µg/cell ± 2.95×10^{-4} µg/cell) and the lowest amount when the TGFβ2 concentration was 0.1 ng/ml (2.45×10^{-4} µg/cell ± 1.58×10^{-5} µg/cell). Moreover, a significant main effect was identified ($p < 0.05$) for

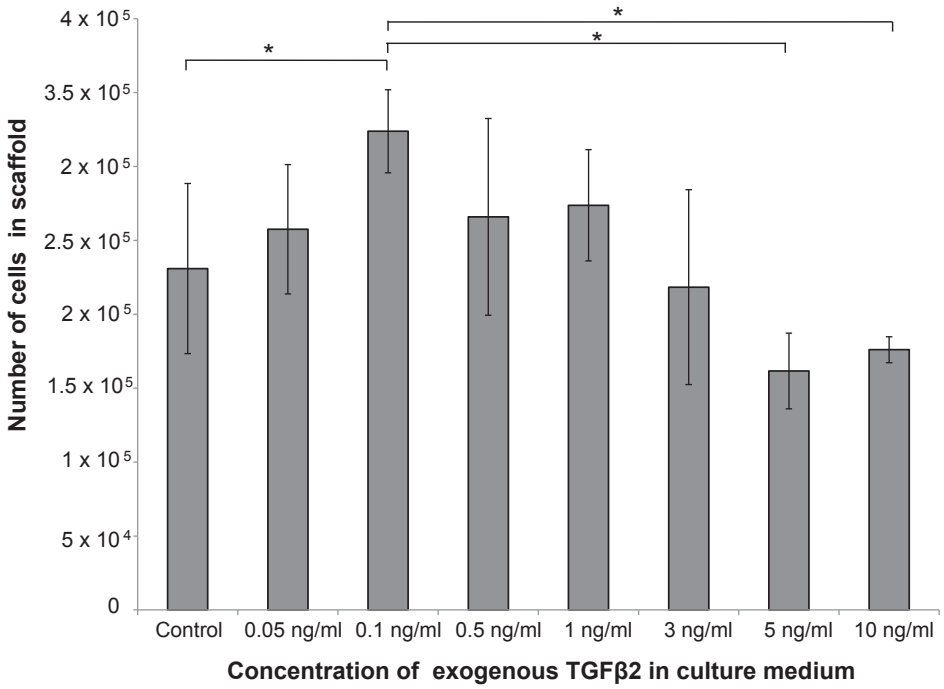

Fig. 4. Cell proliferation results after 7 days post seeding in 80:20 G:F electrospun scaffolds, when different concentrations of exogenous TGFβ2 were added to the culture medium. Average cell number per scaffold is reported for the 8 different culture conditions. Error bars shown are standard deviation ($^*p < 0.05$; $n = 6$).

5 ng/ml and 10 ng/ml compared with the control (1.11×10^{-3} μg/cell ± 5.42×10^{-5} μg/cell, 2.19×10^{-3} μg/cell ± 2.95×10^{-4} μg/cell vs. 3.63×10^{-4} μg/cell ± 6.62×10^{-5} μg/cell).

4. Discussion

Our results suggest that scaffolds composed of 80:20 G:F are more suitable for SMCs growth in both early (2 days) and later (7 days) stages in culture, since cells have shown to adhere and proliferate more compared with 100 G and 50:50 G:F (Figs. 2 and 3). We found a differential effect of TGFβ2 concentration on the SMCs growing in 80:20 G:F sheets. When these constructs were treated with TGFβ2 at concentrations ≤1 ng/ml the cell proliferation and migration increased, and the collagen production was not significantly affected. In contrast, when the constructs were treated with high TGFβ2 concentrations (>1 ng/ml), cell proliferation and migration decreased and the collagen production increased (Figs. 4, 5 and 6).

In the work of Balasubramanian et al., 2013 [16], the authors studied cell growth in scaffolds with a composition of 80% gelatin-20% fibrinogen and 60% gelatin-30% fibrinogen compared to constructs made of 100% fibrinogen. Their findings stated that the addition of gelatin to the fibrinogen scaffolds is beneficial for cell growth since their constructs with 80:20 G:F composition were more likely to cause better cell attachment [16]. When looking closer at our results for differences in proliferation between the scaffolds after 2 and 7 days, it is possible to observe that at 2 days post seeding 100 G flat sheets had a higher number of cells attached than 50:50 G:F. In contrast, at 7 days 100 G scaffolds showed the lowest number of cells growing in the scaffold (Fig. 2). This could indicate that gelatin may be more suitable for cell attachment while fibrinogen may help to promote cell proliferation. It is possible to attribute these results to the fact that gelatin is partially hydrolyzed collagen which preserves the arginine-glycine-aspartic acid (RGD) sequence along its structure [30,31]. This particular amino acid sequence is a specific integrin location for focal adhesion which encourages cell attachment [30–32]. Furthermore, it has been strongly suggested that fibrinogen and its degradation products can stimulate mitotic DNA synthesis and subsequent proliferation. Thus fibrinogen has been considered a mitogenic stimulus [16,33–36].

Cell infiltration results show that SMCs can migrate through the fibrous scaffold, and that migration is progressive along the time in culture, with more than 90% of the scaffold thickness infiltrated after 7 days post seeding (Fig. 3a). A representative image of the cell seeded scaffolds is shown in Fig. 3b, where cells that were homogenously placed on top of the flat sheets are located in different points in the depth of the construct. It is well known that porosity and fiber diameter affect cell migration in electrospun scaffolds. Generally, cell seeded electrospun scaffolds with a percentage of porosity higher than 35% allow adequate migration [37–39]. In the work of Rnjak-Kovacina et al. (2011), the authors demonstrated that fibroblasts seeded in electrospun synthetic human elastin was improved when the porosity of the constructs was increased from 14.5 ± 0.8% to 34.4 ± 1.3%. The authors also observed that in the upper limit of porosity, at 3 days post-seeding the cells had migrated half way through the scaffold and by day 8 they spanned the entire scaffold [37]. From the characterization of our electrospun gelatin-fibrinogen sheets, we found that the fiber diameter was comparable among the different scaffold composition, and the porosities range from 45% to 79% (Table 1), which did not affect cell migration as seen in Fig. 3a. Our results are consistent with that of Rnjak-Kovacina et al. (2011) observations, since at 2 days our SMCs had migrated between 35% and 45% of the construct and at 7 days cell migration was between 90% and 97%.

Our findings on the effect of exogenous TGFβ2 for 7 days in culture suggest that different concentrations can produce different effect on cell proliferation, migration and collagen production. A positive effect on cell proliferation was observed when TGFβ2 was added at the more physiological concentrations of ≤1 ng/ml, with the highest SMCs growth detected at 0.1 ng/ml (Fig. 4). Nevertheless, when the culture medium was supplemented with higher, more super-physiological TGFβ2 concentrations (>1 ng/ml), cell proliferation

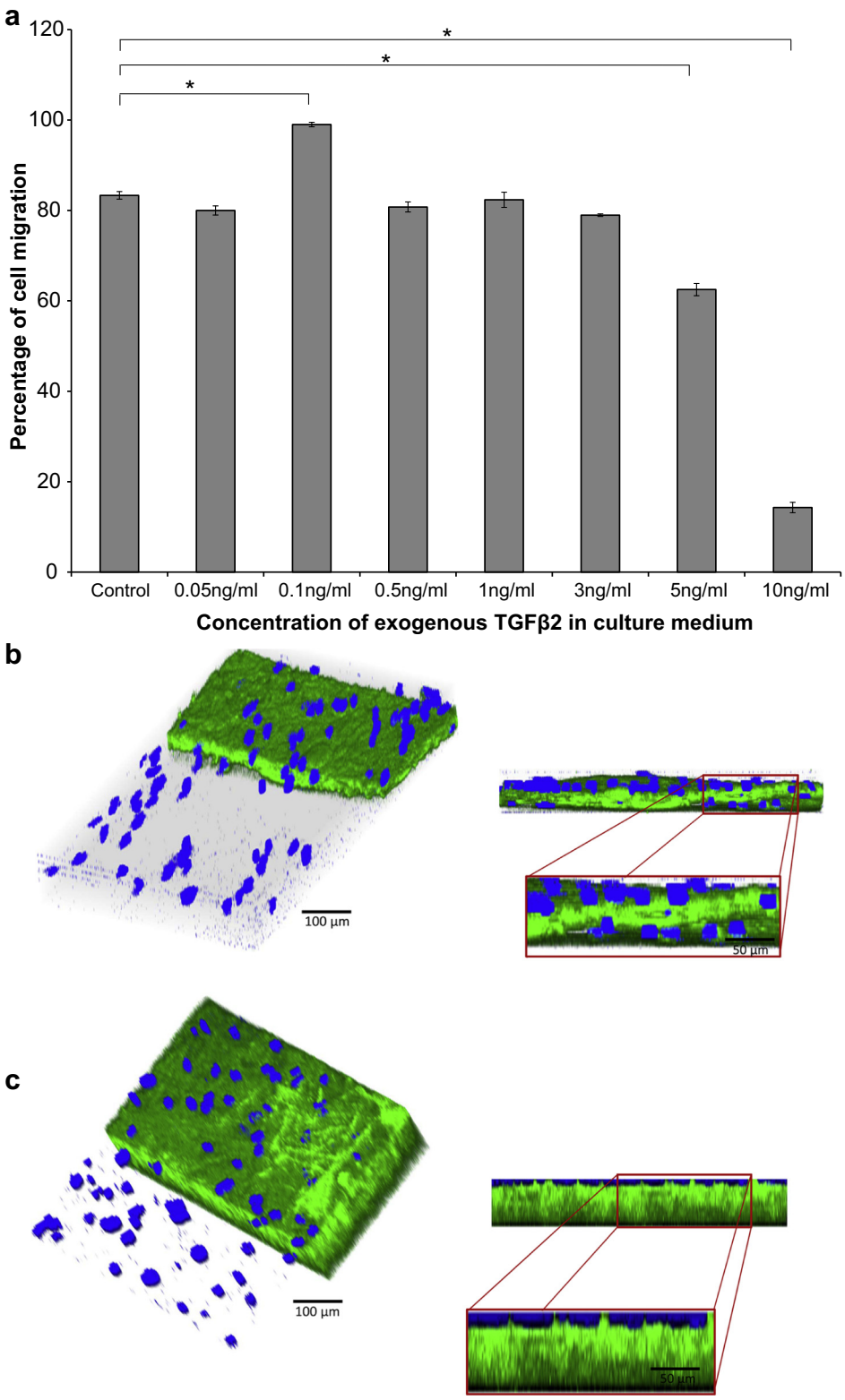

Fig. 5. a) Cell infiltration results after 7 days post seeding in 80:20 G:F electrospun scaffolds, when different concentrations of exogenous TGFβ2 were added to the culture medium. Percentage of migration through the scaffold depth is reported for the 8 different TGFβ2 concentrations. Error bars shown are standard deviation ($^*p < 0.05$; $n = 2$). Representative multiphoton images of an 80:20 G:F flat sheet with cells after 7 days in culture when the concentration of TGFβ2 in culture media was b) 0.1 ng/ml, and c) 10 ng/ml. The material fibers are shown in green, and cell nuclei in blue. In the left image a 3D render of the scaffold is shown with the *y* plane clipped for the green channel. The right image is the *xz* view of the 3D render. The image was acquired at a magnification of 20×.

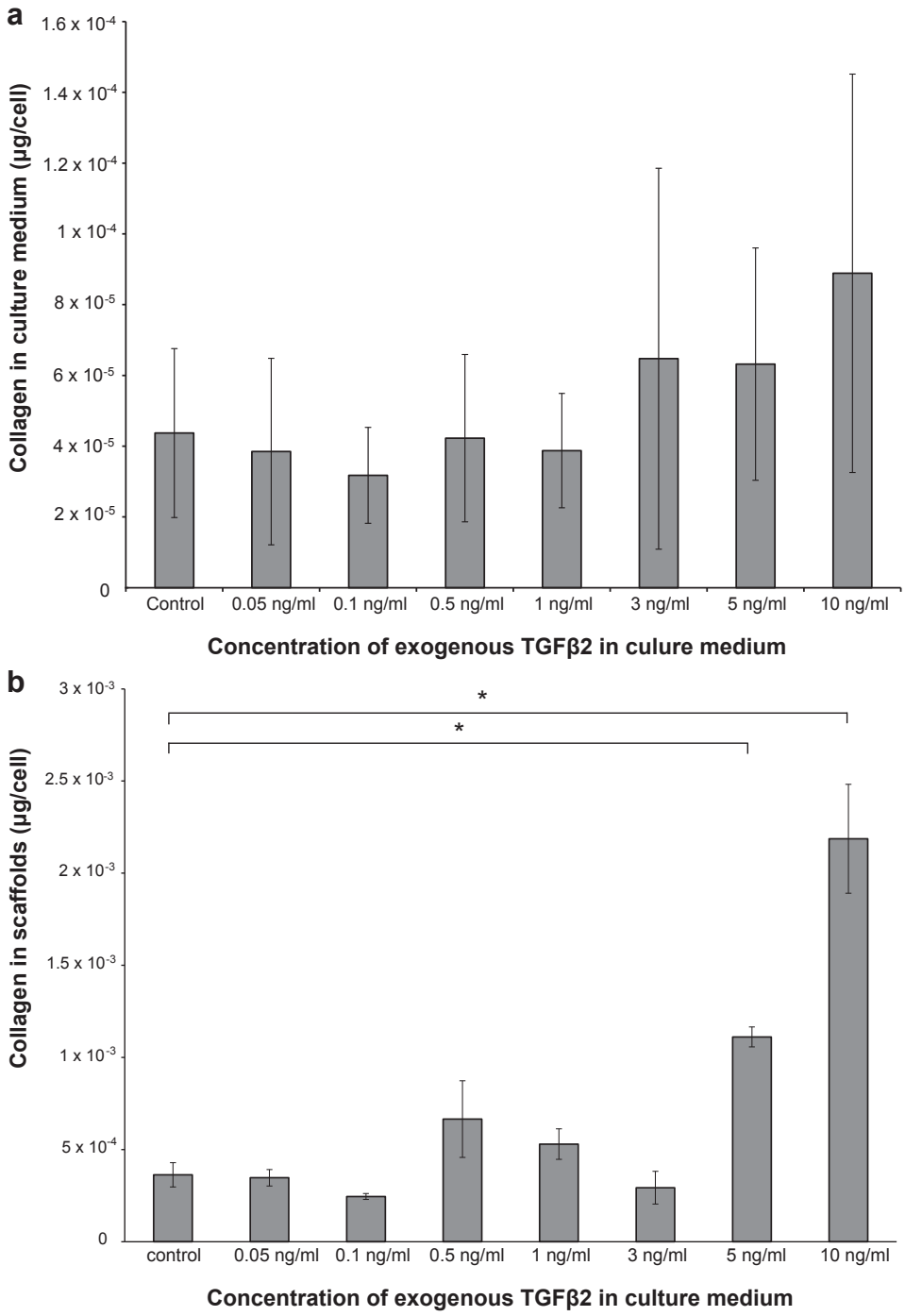

Fig. 6. Collagen produced by SMCs growing on 80:20 G:F electrospun scaffolds, when different concentrations of exogenous TGFβ2 were added to the culture medium. a) Average amount of collagen/cell dissolved in culture medium. Dissolved collagen was assessed over 24 h from day 6 to day 7 after cell seeding. b) Average amount of collagen/cell deposited in the scaffolds after 7 days in culture. Error bars shown are standard deviation ($^*p < 0.05$; $n = 6$).

seemed to be inhibited with the lowest cell count obtained at 5 ng/ml and 10 ng/ml (Fig. 4). A similar trend was found in our cell infiltration results, where the highest and lowest scaffold infiltration was achieved when TGFβ2 was at 0.1 ng/ml and 10 ng/ml, respectively (Fig. 5a). At 0.1 ng/ml TGFβ cells migrated through 99% of the scaffold and were spread out along the *z* axis (Fig. 5b). Conversely, at a concentration of 10 ng/ml TGFβ the cells only migrated through approximately 14% of the flat sheet (in the *z* axis direction), mainly remaining superficial (Fig. 5a and b). Interestingly, when observing the influence of TGFβ2 on collagen production, a direct opposite outcome was found, with a negligible or negative effect obtained with TGFβ2 at concentrations $\leq$1 ng/ml, and a positive effect when TGFβ2 was at concentrations >1 ng/ml (Fig. 6). Contrary to what was found for proliferation and migration, the highest collagen amount (in both the growth medium and in the scaffolds), was obtained with 10 ng/ml TGFβ2, and the lowest for 0.1 ng/ml TGFβ2.

It is well known that SMCs can modulate from a mature or contractile phenotype, which is exhibited in mature tissue, to a

Table 1
Percentage of porosity and fiber diameter for the three different composition of gelatin-fibrinogen electrospun scaffolds. 100% gelatin (100 G), 80% gelatin – 20% fibrinogen (80:20 G:F), 50% gelatin – 50% fibrinogen (50:50 G:F). The values for porosity and fiber diameter were averaged based performed by three separate individuals to minimize any user bias of the manually image thresholding.

Scaffold composition	Percentage of porosity	Fiber diameter
100 G	70.6% ± 14%	3.57 μm ± 1.66 μm
80: 20 G:F	45.4% ± 1.5%	3.82 μm ± 2.04 μm
50:50 G:F	62.3% ± 5.0%	4.48 μm ± 1.56 μm

proliferative or synthetic phenotype, found in new born arteries or under conditions such as injury or atherogenesis [29,40]. In the contractile phenotype these cells have a low rate of proliferation, produce small amounts of ECM, and due to their contractile function, are less able to migrate [29,40,41]. In contrast, when SMCs are in a synthetic phenotype they are highly proliferative, are able to migrate and synthesize ECM [29,40]. It has been demonstrated that SMCs can change between phenotypes depending on different environmental stimuli such as the concentration of TGFβ, which in fact is a key signaling factor for inducing, maintaining, or switching between SMCs phenotypes [41–44]. Depending on its concentration, TGFβ is capable of either promoting or inhibiting SMCs proliferation [45,46]. At low concentrations, TGFβ can stimulate SMC proliferation by promoting platelet-derived growth factor (PDGF), which increases DNA synthesis [45–47]. However, at high TGFβ concentrations the expression of PDGF is down-regulated, causing a reduction in SMCs proliferation [45]. Additionally, when SMCs are exposed to higher concentrations of TGFβ2, this growth factor can also induce proteins such as alpha-smooth muscle actin and desmin, typical of the contractile phenotype [29,41]. In physiological conditions, SMCs in the contractile phenotype proliferate at an extremely low rate, and the production of ECM components such as collagen is low [29,41,43]. Nevertheless in the study of Kubota et al. (2003), the authors validated that the treatment of vascular SMCs with a high concentration of TGFβ1 (10 ng/ml) stimulated collagen synthesis and increased the level of collagen type I mRNA around 2 fold [48]. In a different study, Mann et al., 2001 showed that the use of TGFβ1 can increase the synthesis of ECM components on RGD-containing systems such as gelatin scaffolds [49]. In the context of these TGFβ1 studies, our results would suggest that super-physiologically high TGFβ2 concentrations may be inducing signaling for ECM production through a TGFβ1 pathway [50]. Similar to our results, current literature indicates that when SMCs are exposed to low TGFβ2 concentrations, proliferation is promoted; and when SMCs are exposed to high concentrations of TGFβ2, proliferation is decreased, the contractile phenotype may be induced, and the production of ECM is stimulated [41,45,46,48].

Our study was based on PAOSMCs, however our results can be translated to humans since human and porcine vascular smooth muscle cells (VSMC) have a comparable rate of proliferation, and have shown similar responses to various stimuli *in vitro* [51–56]. Additionally, it has been demonstrated that the biological analogies that establish the pig as physiologically the nearest animal to man, make swine potentially a good model for biomedical research [57,58]. One of the fields in which the pig will make its greatest contribution to human health is that of cardiovascular and circulatory research [57]. The distribution of blood supply by the coronary arteries is almost identical to that of humans, as well as the size of the heart and blood vessels [58].

One limitation of our study was the variability of the thickness of the sheets due to the inherent randomness of the electrospinning process. Our infiltration results had to be normalized by the flat sheet depth and then averaged with the aim of reducing the error introduced by the variability of the scaffold dimensions. Another limitation of the study included the sheets imaging under the multiphoton microscope being unable to capture the second harmonic generation (SHG) signal expected from the collagen produced by the cells. This led us the uncertainty of whether or not the collagen deposited was effectively assembled into a fibrillar form, or if the SHG signal was too low to be detectable by the photomultiplier tube (PMT) in the multiphoton microscope. We demonstrated by using a chemical reaction that SMCs growing in the scaffolds were synthesizing collagen, and also that this synthesis was affected when the cells were treated with different concentrations of TGFβ2. However, our results do not allow us to ensure that this collagen may be fibrillar as it is normally in soft tissue. Future studies will be focused on finding a strategy that allows us to assess if the collagen deposited by the SMCs in the electrospun flat sheets is in fact fibrillar collagen. Additionally, since the autofluorescence signal from the constructs is much higher than the fluorescence signal from the antibodies, our attempts to image SMCs growing in the flat sheets using ICC were not successful. This prevents us from obtaining important information about morphology and the expression levels of proteins related to SMC phenotype. In order to be able to image SMCs growing in gelatin-fibrinogen constructs using ICC, it would be necessary to strategically increase the signal from the secondary antibodies. Our laboratory is currently investigating if increased culture time for both antibodies will improve the fluorophore signal enough to quantify SMC morphology in the constructs. Our observations suggest that high concentrations of TGFβ2 induce an ECM producing contractile-like SMC phenotype; nevertheless, morphology and protein marker expression should be used to confirm these results. Since it is important to gain knowledge on how SMC phenotype is affected by a TGFβ stimulus, our future research will focus on the assessment of morphology and the expression levels of proteins such as alpha-smooth muscle actin, calponin, smooth muscle myosin heavy chain, and caldesmon [41]. Furthermore, as part of the study of the tissue engineered scaffolds, our future work will also involve the biomechanical characterization of electrospun sheets seeded with SMCs and treated with exogenous TGFβ2 at different concentrations. The biomechanical response will be measured using a microbiaxial optomechanical device (MOD) designed in our laboratory to simultaneously measure the macroscopic and microstructural properties of planar and tubular vascular tissues [22,59,60].

5. Conclusions

Electrospun scaffolds composed of 80% gelatin and 20% fibrinogen are attractive for SMC growth and migration, since gelatin facilitates cell attachment and fibrinogen seems to promote cell proliferation. When our tissue-engineered scaffolds were treated with TGFβ2, a differential modulation was observed depending on the concentration, noticing that at low concentrations of TGFβ2 (≤1 ng/ml) cell proliferation was enhanced with no significant effect on cell infiltration and collagen production. Increasing the concentration of TGFβ2 above 1 ng/ml has an opposite effect on the cell behavior, where the mitotic function was lower, the migration was minimal, and the collagen production was increased. According to these results it is possible to propose a strategy that we call "T\the TGFβ2 switch" to biochemically control SMC function growing in tissue engineered scaffolds: in early stages, SMC proliferation and migration will be promoted by treating the cells with low concentrations of TGFβ2, ideally 0.1 ng/ml, as it has been demonstrated in this work. Subsequently, once the cells are distributed throughout the scaffold, the concentration of TGFβ2

will be significantly increased to 10 ng/ml with the aim of promoting collagen production and possibly induce the contractile phenotype. Future research in our laboratory will further explore the implementation of "the TGFβ2 switch" strategy, evaluating cell proliferation, infiltration, collagen production and phenotype shifting of SMCs growing in 8:20 G:F electrospun scaffolds. Additionally, we will focus on exploring the effect of simultaneous biomechanical and biochemical stimulation on the growth and development of gelatin based vascular constructs.

Acknowledgments

This research was funded by the NIH (NHLBI-1R21HL111990-01A1 to JPVG). Imaging was performed on an NIH sponsored shared device NIH/NCRRS10RR023737.

References

[1] Fuchs JR, Nasseri BA, Vacanti JP. Tissue engineering: a 21st century solution to surgical reconstruction. Ann Thorac Surg 2001;72:577–91.
[2] Langer R, Vacanti JP. Tissue engineering. Science 1993;260:920–6.
[3] O'Brien FJ. Biomaterials & scaffolds for tissue engineering. Mater Today 2011;14:88–95.
[4] Vacanti JP, Langer R. Tissue engineering: the design and fabrication of living replacement devices for surgical reconstruction and transplantation. Lancet 1999;354:S32–4.
[5] Chen Q-Z, Harding SE, Ali NN, Lyon AR, Boccaccini AR. Biomaterials in cardiac tissue engineering: ten years of research survey. Mater Sci Eng R 2008;59:1–37.
[6] Gunatillake PA, Adhikari R. Biodegradable synthetic polymers for tissue engineering. Eur Cell Mater 2003;5:1–16.
[7] Dhandayuthapani B, Yoshida Y, Maekawa T, Kumar DS. Polymeric scaffolds in tissue engineering application: a review. Int J Polym Sci 2011;2011.
[8] Nikolovski J, Mooney DJ. Smooth muscle cell adhesion to tissue engineering scaffolds. Biomaterials 2000;21:2025–32.
[9] Kohane DS, Langer R. Polymeric biomaterials in tissue engineering. Pediatr Res 2008;63:487–91.
[10] Oh SH, Lee JH. Hydrophilization of synthetic biodegradable polymer scaffolds for improved cell/tissue compatibility. Biomed Mater 2013;8:014101.
[11] Sell SA, Wolfe PS, Garg K, McCool JM, Rodriguez IA, Bowlin GL. The use of natural polymers in tissue engineering: a focus on electrospun extracellular matrix analogues. Polymers 2010;2:522–53.
[12] Mano J, Silva G, Azevedo HS, Malafaya P, Sousa R, Silva S, et al. Natural origin biodegradable systems in tissue engineering and regenerative medicine: present status and some moving trends. J R Soc Interface 2007;4:999–1030.
[13] Marler JJ, Upton J, Langer R, Vacanti JP. Transplantation of cells in matrices for tissue regeneration. Adv Drug Deliv Rev 1998;33:165–82.
[14] Lannutti J, Reneker D, Tea Ma, Tomasko D, Farson D. Electrospinning for tissue engineering scaffolds. Mater Sci Eng C 2007;27:504–9.
[15] Rim NG, Shin CS, Shin H. Current approaches to electrospun nanofibers for tissue engineering. Biomed Mater 2013;8:014102.
[16] Balasubramanian P, Prabhakaran MP, Kai D, Ramakrishna S. Human cardiomyocyte interaction with electrospun fibrinogen/gelatin nanofibers for myocardial regeneration. J Biomater Sci Polym Ed 2013;24:1660–75.
[17] Molin DG, DeRuiter MC, Wisse LJ, Azhar M, Doetschman T, Poelmann RE, et al. Altered apoptosis pattern during pharyngeal arch artery remodelling is associated with aortic arch malformations in Tgfβ2 knock-out mice. Cardiovasc Res 2002;56:312–22.
[18] Azhar M, Brown K, Gard C, Chen H, Rajan S, Elliott DA, et al. Transforming growth factor Beta2 is required for valve remodeling during heart development. Dev Dyn 2011;240:2127–41.
[19] Gallicchio MA. Culture of human smooth muscle cells. Atherosclerosis 2001;(Springer):137–46.
[20] Gotlieb AI, Boden P. Porcine aortic organ culture: a model to study the cellular response to vascular injury. In Vitro 1984;20:535–42.
[21] Williams MJ, Utzinger U, Barkmeier-Kraemer JM, Geest JPV. Differences in the microstructure and biomechanical properties of the recurrent laryngeal nerve as a function of age and location. J Biomech Eng 2014;136:081008.
[22] Haskett D, Azhar M, Utzinger U, Geest JPV. Progressive alterations in microstructural organization and biomechanical response in the ApoE mouse model of aneurysm. Biomatter 2013;3.
[23] Chen X, Nadiarynkh O, Plotnikov S, Campagnola PJ. Second harmonic generation microscopy for quantitative analysis of collagen fibrillar structure. Nat Protoc 2012;7:654–69.
[24] Lee SH, Hungerford JE, Little CD, Iruela-Arispe ML. Proliferation and differentiation of smooth muscle cell precursors occurs simultaneously during the development of the vessel wall. Dev Dyn 1997;209:342–52.
[25] Long X, Slivano OJ, Cowan SL, Georger MA, Lee T-H, Miano JM. Smooth muscle calponin an unconventional CArG-dependent gene that antagonizes neointimal formation. Arterioscler Thromb Vasc Biol 2011;31:2172–80.
[26] Hughes S, Chan-Ling T. Characterization of smooth muscle cell and pericyte differentiation in the rat retina in vivo. Invest Ophthalmol Vis Sci 2004;45:2795–806.
[27] Calponin El-Mezgueldi M. Int J Biochem Cell Biol 1996;28:1185–9.
[28] Skalli O, Pelte M, Peclet M, Gabbiani G, Gugliotta P, Bussolati G, et al. Alpha-smooth muscle actin, a differentiation marker of smooth muscle cells, is present in microfilamentous bundles of pericytes. J Histochem Cytochem 1989;37:315–21.
[29] Rensen S, Doevendans P, Van Eys G. Regulation and characteristics of vascular smooth muscle cell phenotypic diversity. Neth Heart J 2007;15:100–8.
[30] Wu S-C, Chang W-H, Dong G-C, Chen K-Y, Chen Y-S, Yao C-H. Cell adhesion and proliferation enhancement by gelatin nanofiber scaffolds. J Bioact Compat Pol 2011;26:565–77.
[31] Rungsiyanont S, Dhanesuan N, Swasdison S, Kasugai S. Evaluation of biomimetic scaffold of gelatin–hydroxyapatite crosslink as a novel scaffold for tissue engineering: biocompatibility evaluation with human PDL fibroblasts, human mesenchymal stromal cells, and primary bone cells. J Biomatter Appl 2012;27:47–54.
[32] Rosellini E, Cristallini C, Barbani N, Vozzi G, Giusti P. Preparation and characterization of alginate/gelatin blend films for cardiac tissue engineering. J Biomed Mater Res A 2009;91:447–53.
[33] Gardiner EE, D'Souza SE. A mitogenic action for fibrinogen mediated through intercellular adhesion molecule-1. J Biol Chem 1997;272:15474–80.
[34] Moiseeva EP. Adhesion receptors of vascular smooth muscle cells and their functions. Cardiovasc Res 2001;52:372–86.
[35] Sturge J, Carey N, Davies AH, Powell JT. Fibrin monomer and fibrinopeptide B act additively to increase DNA synthesis in smooth muscle cells cultured from human saphenous vein. J Vasc Surg 2001;33:847–53.
[36] Ishida T, Tanaka K. Effects of fibrin and fibrinogen-degradation products on the growth of rabbit aortic smooth muscle cells in culture. Atherosclerosis 1982;44:161–74.
[37] Rnjak-Kovacina J, Wise SG, Li Z, Maitz PK, Young CJ, Wang Y, et al. Tailoring the porosity and pore size of electrospun synthetic human elastin scaffolds for dermal tissue engineering. Biomaterials 2011;32:6729–36.
[38] Lee JB, Jeong SI, Bae MS, Yang DH, Heo DN, Kim CH, et al. Highly porous electrospun nanofibers enhanced by ultrasonication for improved cellular infiltration. Tissue Eng Part A 2011;17:2695–702.
[39] Horst M, Milleret V, Nötzli S, Madduri S, Sulser T, Gobet R, et al. Increased porosity of electrospun hybrid scaffolds improved bladder tissue regeneration. J Biomed Mater Res A 2014;102:2116–24.
[40] Worth NF, Rolfe BE, Song J, Campbell GR. Vascular smooth muscle cell phenotypic modulation in culture is associated with reorganisation of contractile and cytoskeletal proteins. Cell Motil Cytoskelet 2001;49:130–45.
[41] Beamish JA, He P, Kottke-Marchant K, Marchant RE. Molecular regulation of contractile smooth muscle cell phenotype: implications for vascular tissue engineering. Tissue Eng 2010;16:467–91.
[42] Owens GK. Regulation of differentiation of vascular smooth muscle cells. Physiol Rev 1995;75:487–517.
[43] Owens GK, Kumar MS, Wamhoff BR. Molecular regulation of vascular smooth muscle cell differentiation in development and disease. Physiol Rev 2004;84:767–801.
[44] Spin JM, Maegdefessel L, Tsao PS. Vascular smooth muscle cell phenotypic plasticity: focus on chromatin remodelling. Cardiovasc Res 2012;95:147–55.
[45] Moses MA, Klagsbrun M, Shing Y. The role of growth factors in vascular cell development and differentiation. Int Rev Cyto 1995;161:1–48.
[46] Stegemann JP, Nerem RM. Phenotype modulation in vascular tissue engineering using biochemical and mechanical stimulation. Ann Biomed Eng 2003;31:391–402.
[47] Guo X, Chen S-Y. Transforming growth factor-β and smooth muscle differentiation. World J Biol Chem 2012;3:41.
[48] Kubota K, Okazaki J, Louie O, Kent KC, Liu B. TGF-β stimulates collagen (I) in vascular smooth muscle cells via a short element in the proximal collagen promoter. J Surg Res 2003;109:43–50.
[49] Mann BK, Schmedlen RH, West JL. Tethered-TGF-β increases extracellular matrix production of vascular smooth muscle cells. Biomaterials 2001;22:439–44.
[50] Blanchette F, Day R, Dong W, Laprise M, Dubois C. TGFbeta1 regulates gene expression of its own converting enzyme furin. J Clin Invest 1997;99:1974.
[51] Brisset AC, Hao H, Camenzind E, Bacchetta M, Geinoz A, Sanchez J-C, et al. Intimal smooth muscle cells of porcine and human coronary artery express S100A4, a marker of the rhomboid phenotype in vitro. Circ Res 2007;100:1055–62.
[52] Burnstock G. Purinergic signaling and vascular cell proliferation and death. Arterioscler Thromb Vasc Biol 2002;22:364–73.
[53] Corrêa-Giannella ML, de Azevedo MRA, Leroith D, Giannella-Neto D. Fibronectin glycation increases IGF-I induced proliferation of human aortic smooth muscle cells. Diabetol Metab Syndr 2012;4.
[54] Gollasch M, Ried C, Bychkov R, Luft FC, Haller H. K+ currents in human coronary artery vascular smooth muscle cells. Circ Res 1996;78:676–88.

[55] Hao H, Gabbiani G, Bochaton-Piallat M-L. Arterial smooth muscle cell heterogeneity implications for atherosclerosis and restenosis development. Arterioscler Thromb Vasc Biol 2003;23:1510–20.
[56] Patel S, Shi Y, Niculescu R, Chung EH, Martin JL, Zalewski A. Characteristics of coronary smooth muscle cells and adventitial fibroblasts. Circulation 2000;101:524–32.
[57] Swindle M, Makin A, Herron A, Clubb F, Frazier K. Swine as models in biomedical research and toxicology testing. Vet Pathol 2012;49:344–56.
[58] Douglas WR. Of pigs and men and research. Space Life Sci 1972;3:226–34.
[59] Keyes JT, Borowicz SM, Rader JH, Utzinger U, Azhar M, Vande Geest JP. Design and demonstration of a microbiaxial optomechanical device for multiscale characterization of soft biological tissues with two-photon microscopy. Microsc Microanal 2011;17:167–75.
[60] Keyes JT, Haskett DG, Utzinger U, Azhar M, Geest JPV. Adaptation of a planar microbiaxial optomechanical device for the tubular biaxial microstructural and macroscopic characterization of small vascular tissues. J Biomech Eng 2011;133:075001.